Concerted Proton–Electron Transfers. Consistency between Electrochemical Kinetics and their Homogeneous Counterparts

ARTICLE *in* JOURNAL OF THE AMERICAN CHEMICAL SOCIETY · NOVEMBER 2011

Impact Factor: 12.11 · DOI: 10.1021/ja206561n · Source: PubMed

JACS
JOURNAL OF THE AMERICAN CHEMICAL SOCIETY

ARTICLE

pubs.acs.org/JACS

Concerted Proton−Electron Transfers. Consistency between Electrochemical Kinetics and their Homogeneous Counterparts.

Cyrille Costentin, Viviane Hajj, Cyril Louault, Marc Robert, and Jean-Michel Savéant*

Univ Paris Diderot, Sorbonne Paris Cité, Laboratoire d'Electrochimie Moléculaire, Unité Mixte de Recherche Univ - CNRS No 7591, Bâtiment Lavoisier, 15 rue Jean de Baïf, 75205 Paris Cedex 13, France

Supporting Information

ABSTRACT: The concerted proton−electron transfer (CPET) oxidation of phenol with water (in water) and hydrogen phosphate as proton acceptors provides a good example for testing the consistency of the electrochemical and homogeneous approaches to a reaction, the comprehension of which raises more mechanistic and kinetic challenges than that of a simple outer-sphere electron transfer. Comparison of the intrinsic kinetic characteristics (obtained at zero driving force of the CPET reaction) shows that consistency is indeed observed after a careful identification and quantitation of side factors (electrical work terms, image force effects). Water (in water) appears as a better intrinsic proton acceptor than hydrogen phosphate in both cases in terms of reorganization energy and pre-exponential factor, corroborating the mechanism by which electron transfer is concerted with Grotthus-type proton translocation in water. Detailed compared analysis of the approaches also revealed that modest but significant electric field effects may be at work in the electrochemical case. Comparison with phenoxide ion oxidation, taken as a reference outer-sphere electron transfer, points to a CPET precursor complex that possesses a precise spatial structure allowing the formation of one or several H-bonds as required by the occurrence of the CPET reaction, thus decreasing considerably the number of efficient collisions compared with those undergone by structureless spherical reactants.

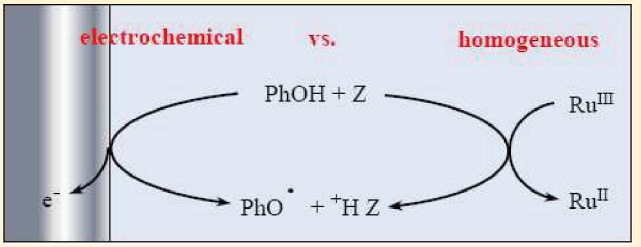

INTRODUCTION

Association between electron and proton transfers is ubiquitous in natural and artificial systems. It is also likely to interfere in reactions currently envisaged for the resolution of contemporary energy challenges. These proton-coupled electron transfers (PCETs) may follow stepwise or concerted pathways or both[1] as illustrated in Scheme 1 with the example of phenol oxidation. Concerted pathways (CPET[2]) skip the high-energy intermediates involved in the two stepwise pathways, PET (proton transfer followed by electron transfer) and EPT (electron transfer followed by proton transfer). They may therefore be more advantageous if the likely additional kinetic cost is not too high. Although the concerted−stepwise competition is a completely general issue, oxidation of phenols has been taken repeatedly as an illustrating example keeping in mind the prominent role they play in reactions occurring in natural systems particularly, but not exclusively, in the oxidation of a tyrosine (Tyr_z) in photosystem II.[1,3]

Establishment of the reaction mechanism and analysis of the kinetic characteristics have been tackled from two sides, usual homogeneous kinetics, where the electron donor or acceptor is present in solution, on the one hand, and electrochemical kinetics where electron transfer takes place at the electrode surface, on the other. Most homogeneous kinetic studies usually consider electrochemistry merely as a way to access "redox potentials", actually standard (or formal) potentials, rather than a source of kinetic and mechanistic information. This state of affairs has two drawbacks in the case where the system does not give rise to a reversible diffusion-controlled electrochemical response. One is that the "redox potentials" thus obtained may not be a good estimate of the sought standard (or formal) potentials.[4] The second is that the available kinetic and mechanistic information is not exploited despite the fact that the kinetic models used in both areas are basically the same after taking due account of the heterogeneous character of the electrochemical reactions and hence of the interference of reactant transport in the overall kinetics.

These considerations are particularly true in the field of proton-coupled electron transfers where both homogeneous and electrochemical approaches have been applied to the same systems, although systematic comparisons are scarce. The discussion below aims at illustrating the consistency of the two approaches with the example of the oxidation of phenol with water (in water) and hydrogen phosphate as proton acceptors and detailing the factors that should be taken into account to make the comparison between them meaningful. Homogeneous oxidation with water (in water) and hydrogen phosphate as proton acceptors has already given rise to a detailed study.[5] This is also the case for the electrochemical oxidation of phenol with water (in water) as proton acceptor.[6] What is lacking at present to proceed to the comparison between the two approaches is data concerning the

Received: July 14, 2011
Published: November 09, 2011

Scheme 1. PCET Stepwise (Blue) and Concerted (Red) Pathways

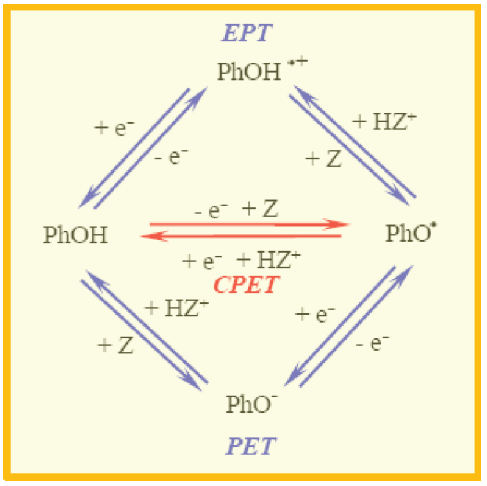

electrochemical oxidation of phenol with hydrogen phosphate as proton acceptor. This will be the object of the first part of the following Results section. Electrochemical work terms will then be seen to play an important role in the achievement of an accurate comparison, calling for the determination of the potential difference between the reaction site and the solution. This is described in the second part of the Results section together with the ensuing correction of the standard rate constant. Other results of interest for the analysis of the PCET reaction concern the oxidation of phenoxide ion, which may serve as a pure ET reference in the analysis of phenol oxidation. This is described in the third part of the Results section. The Discussion section will be devoted to testing the consistency of the homogeneous and electrochemical approaches based on the whole set of experimental results. In both cases, the *intrinsic* CPET reactivities when water (in water) and hydrogen phosphate are the proton acceptors are compared. Hydrogen phosphate is a stronger base than water. This obvious thermodynamical advantage makes the CPET reaction *extrinsically* faster in the first case than in the second. Concerning the intrinsic reactivities, derived from the standard rate constants in the electrochemical case and from the self-exchange rate constants in the homogeneous case, the picture is reversed. It will be indeed seen that water (in water) appears as a better intrinsic proton acceptor than hydrogen phosphate, consistently in the electrochemical and homogeneous cases.

RESULTS

Electrochemical Oxidation of Phenol with Hydrogen Phosphate As Proton Acceptor. Previous cyclic voltammetric studies carried out at low scan rates[6,7] allowed the establishment of a Pourbaix diagram (Figure 1), based on the observation that under these conditions, the electrochemical oxidation of phenol involves a fast and reversible proton-coupled electron transfer followed, whatever its mechanism, by a rate-determining dimerization step (Scheme 2). Since the dimerization rate constant was known from previous pulse radiolysis studies ($k_{dim} = 1.3 \times 10^9\ M^{-1}\ s^{-1}$),[8] its effect on the cyclic voltammetric responses could be corrected for so as to obtain the variation of the apparent standard potential of the PhOH/PhO• + H^+ couple with pH as summarized in Figure 1. Standard potentials characterizing each putative proton acceptor

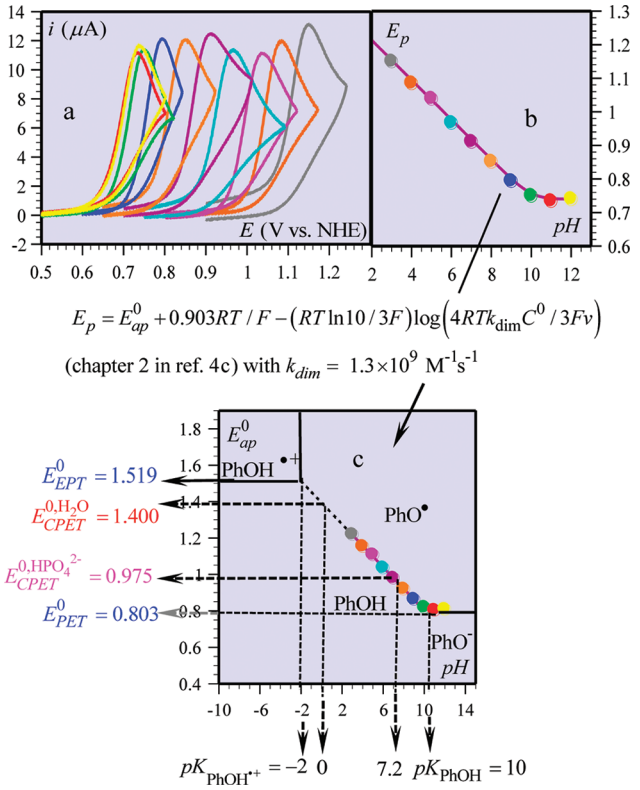

Figure 1. Derivation of the Pourbaix diagram from slow scan cyclic voltammetry: (a) Cyclic voltammetry of 0.2 mM phenol at 0.2 V/s in 0.05 M Britton−Robinson buffers in the presence of 0.5 M KNO_3. (b) Peak potential, E_p, as a function of pH. (c) Pourbaix diagram obtained after correction from the effect of follow-up dimerization according to the equation (E^0_{app}, apparent standard potential; k_{dim}, dimerization rate constant; v, scan rate; C^0, phenol concentration). The various standard potentials derived from the Pourbaix diagram correspond to the pathway indicated as subscript and, in the case of CPET, to the proton acceptor indicated as superscript. All potentials in V vs NHE.

Scheme 2

$$PhOH \xrightleftharpoons[-e^-]{E^0_{app},\ k_S^{app},\ \alpha} H^+ + PhO^\bullet$$

$$2\ PhO^\bullet \xrightarrow{2k_{dim}} dimer$$

could then be gathered (Figure 1c), but, in these conditions, no assignment of the PCET mechanism and characteristic rate constant could be achieved. This was obtained upon raising the scan rate as depicted in Figure 2. The variations of the peak potential with scan rate and phosphate concentration (Figure 3) may be simulated[9] according to the mechanism in Scheme 2 with a Butler−Volmer rate law for electron transfer and a transfer coefficient, $\alpha = 0.5$ (in line with the thickness of the cyclic voltammetric responses):[4c]

$$\frac{i}{FS} = k_S^{app} \exp\left[\frac{F}{2RT}(E - E^0_{app})\right] \times \left(\sum [Red] - \sum [Ox] \exp\left[-\frac{F}{RT}(E - E^0_{app})\right]\right) \quad (1)$$

dx.doi.org/10.1021/ja206561n |J. Am. Chem. Soc. 2011, 133, 19160–19167

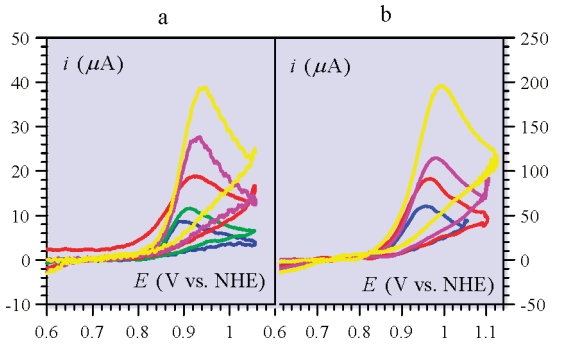

Figure 2. Cyclic voltammetry of 0.2 mM phenol in a phosphate buffer at pH = 7.2 ($[HPO_4^{2-}] = 0.125$ M) in the presence of KNO_3 (0.5 M) as a function of scan rate, from bottom to top: (a) 0.1, 0.2, 0.5, 1, 2; (b) 5, 10, 20, 50 V/s.

where i is the current, S is the electrode surface area, and $\Sigma[\mathrm{Red}]$ and $\Sigma[\mathrm{Ox}]$ are the sums of concentrations of all reduced forms of phenol and all oxidized forms of phenol, respectively (see Scheme 1). The values of the apparent standard potential, E^0_{app}, used in the simulation are those previously obtained at low scan rate under the form of the Pourbaix diagram of Figure 1. The resulting values of the apparent standard rate constant, k_S^{app}, are gathered in Figure 4 for several concentrations of phosphate buffer. The apparent standard rate constant measures the superposition of all pathways, stepwise and concerted, that are represented in Scheme 1, with $Z = H_2O, HO^-, HPO_4^{2-}$. Since the proton transfers in the stepwise pathways are fast, they may be considered as being always at equilibrium. The contribution of the stepwise pathways may therefore be considered as being a function of pH, independently from the particular proton acceptor involved. This is not the case for the CPET pathways, the kinetics of which depends of the nature of the proton acceptor in each case. It follows that (see Supporting Information):

$$k_S^{app} = \frac{k_S^{PET}}{\sqrt{1 + 10^{(pK_{PhOH^{\bullet+}} - pH)}} \times \sqrt{1 + 10^{(pK_{PhOH} - pH)}}} + \frac{k_S^{EPT}}{\sqrt{1 + 10^{(pH - pK_{PhOH^{\bullet+}})}} \times \sqrt{1 + 10^{(pH - pK_{PhOH})}}} + \frac{k_S^{CPET-HPO_4^{2-}} \sqrt{[H_2PO_4^-] \times [HPO_4^{2-}]}/C_S}{\sqrt{1 + 10^{(pK_{PhOH^{\bullet+}} - pH)}} \times \sqrt{1 + 10^{(pH - pK_{PhOH})}}} + \frac{k_S^{CPET-H_2O} \sqrt{([H_3O^+]/C_S)} + k_S^{CPET-HO^-} \sqrt{[HO^-]/C_S}}{\sqrt{1 + 10^{(pK_{PhOH^{\bullet+}} - pH)}} \times \sqrt{1 + 10^{(pH - pK_{PhOH})}}} \quad (2)$$

where C_S is a normalizing concentration taken as equal to 1 M.

The notations for the concerted pathways' standard rate constants are self-explanatory; k_S^{PET} stands for the electron transfer from phenoxide ion in the framework of the PET mechanism and k_S^{EPT} stands for the electron transfer from phenol itself, leading to the cation radical, in the framework of the EPT mechanism. Equation 2 may be rewritten as, noting that the experiments are carried out at pH = 7.2, the pK of hydrogen phosphate:

$$k_S^{app} = k_S^{indep\ HPO_4^{2-}} + \frac{k_S^{CPET-HPO_4^{2-}}}{\sqrt{1 + 10^{(pK_{PhOH^{\bullet+}} - pH)}} \times \sqrt{1 + 10^{(pH - pK_{PhOH})}}} \frac{[HPO_4^{2-}]}{C_S} \quad (3)$$

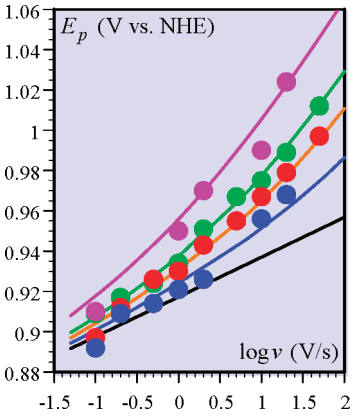

Figure 3. Cyclic voltammetry of 0.2 mM phenol in a phosphate buffer at pH = 7.2 in the presence of 0.5 M KNO_3. Variation of the peak potential with the scan rate, for different buffer concentrations: 0.025, 0.05, 0.25, and 0.5 M (magenta, green, red, and blue dots respectively). Colored lines: simulation for each buffer concentration according to the mechanism in Scheme 2 (see text). Black line: kinetic control by follow-up dimerization.

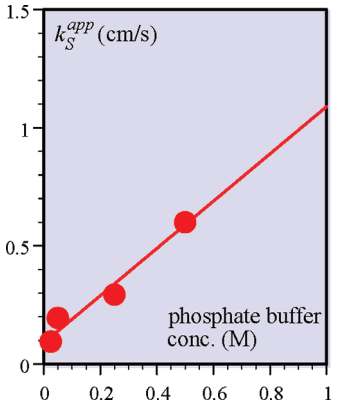

Figure 4. Apparent standard rate constant as a function of phosphate buffer concentration. Full line: representation of eq 3.

so as to make appear a term independent from phosphate concentration, $k_S^{indepHPO_4^{2-}}$, and a term proportional to phosphate concentration. The very fact that the apparent standard rate constant is a unity-slope linear function of phosphate concentration points to the occurrence of a CPET−HPO_4^{2-} pathway. Since the protonation step of the PET and EPT pathways are at equilibrium, the contribution of phosphate to these pathways is independent of its concentration, its role being merely to fix the pH.

Application of eq 3 to the experimental data in Figure 4 provides the value of the constant of interest, $k_S^{CPET-HPO_4^{2-}}$ (Table 1).

Although not central to the determination of $k_S^{CPET-HPO_4^{2-}}$, it is interesting to estimate the relative contributions of the various pathways besides the contribution of the CPET−HPO_4^{2-} pathway. This is obtained by application of eq 2, using the following set of parameters (Table 1), and leading to the diagrams in Figure 5. We note that in the phosphate buffer, the contribution of the CPET−HPO_4^{2-} pathway prevails. Concerning the assumption that the proton transfers in the stepwise pathways are at equilibrium, we may note that in the opposite case, the

Table 1. Electrochemical Standard Rate Constants Characterizing the Various Competing Pathways

pathway	standard rate constants (uncorrected from double layer effects) at 25 °C
PET	$k_S^{PET} = 1$ cm s^{-1} [a]
EPT	$k_S^{EPT} = 1$ cm s^{-1} [b]
CPET−H_2O	$k_S^{CPET-H_2O} = 25$ cm s^{-1} [6]
CPET−D_2O	$k_S^{CPET-D_2O} = 10$ cm s^{-1} [6]
CPET−HO^-	$k_S^{CPET-HO^-} = 25$ cm s^{-1} M^{-1} [c]
CPET−DO^-	$k_S^{CPET-DO^-} \approx 10$ cm s^{-1} M^{-1} [c]
CPET−HPO_4^{2-}	$k_S^{CPET-HPO_4^{2-}} = 1.1$ cm s^{-1} M^{-1}
CPET−DPO_4^{2-}	$k_S^{CPET-DPO_4^{2-}} = 0.4$ cm s^{-1} M^{-1}
Other Parameters (Values at 25 °C)	
pK's	p$K_{PhOH} = 10.0$,[d] p$K_{PhOD} = 10.7$
	p$K_{PhOH^{+\bullet}} = -2$,[10] p$K_{PhOD^{+\bullet}} \approx -1.6$ [e]
	p$K_{H_2PO_4^-} = 7.2$,[11a] p$K_{D_2PO_4^-} = 7.8$[12]
diffusion coefficients (cm^2 s^{-1})	$D_{PhOH} = 3.6 \times 10^{-5}$ [f], $D_{PhOD} = 3.0 \times 10^{-5}$ [f]
dimerization rate constants (M^{-1} s^{-1})	$k_{dim}^{H_2O} = 1.3 \times 10^9$ [13] $k_{dim}^{D_2O} = 1.0 \times 10^9$ [g]

[a] From the cyclic voltammetry of phenoxide ion, see next section. [b] Approximate estimation assuming that solvent reorganization is about the same as in the preceding case, taking into account that a gross estimate is sufficient in view of the smallness of the contribution of this pathway in the pH range of interest (see Figure 5). [c] Assuming that the mechanism of the CPET−H(D)O$^-$ reaction is the exact reverse of the mechanism of the CPET−$H(D)_2O$ reaction. The approximate character of this estimation has no important consequences since the contribution of this pathway is modest, due to the small concentration of HO$^-$ in the pH range of interest (see Figure 5). [d] From the Pourbaix diagram in Figure 1c in agreement with literature data.[11b] [e] Estimated from p$K_D \approx$ pK_H + 0.4.[14] [f] From the CV peak currents. [g] From $k_{dim}^{H_2O}$, corrected by the ratio of the diffusion coefficient.

contributions of the PET and EPT pathway would be less than that pictured in Figure 5, that is, even more negligible.

A similar, albeit simplified, procedure was used to obtained the standard rate constant in D_2O. The variation of the peak potential with scan rate at one concentration of hydrogen phosphate is shown in Figure 6. The apparent standard rate constant was extracted from the data in Figure 6 in the same way, as in Figure 3 using the parameter values listed in Table 1, thus leading to the standard rate constants in the same table.

Work Terms in the Electrochemical Reaction: Double Layer Correction. In the application of the Butler−Volmer law (eq 1) to the electrochemical oxidation of phenol with water and hydrogen phosphate, respectively, works terms that describe the transfer of the reactant from the bulk of the solution to the reaction site, w_R^Z, and of the products from the reaction site to the solution w_P^Z, (Z being either water or hydrogen phosphate), have to be introduced, leading to the following correction of the raw standard rate constant data.

$$k_{S,\,corr}^{CPET-Z} = k_S^{CPET-Z} \exp\left[\frac{F(w_R^Z + w_P^Z)}{2RT}\right]$$

The work terms results from the application of the potential in the reaction site, ϕ_Z, to the charge of reactant and products,

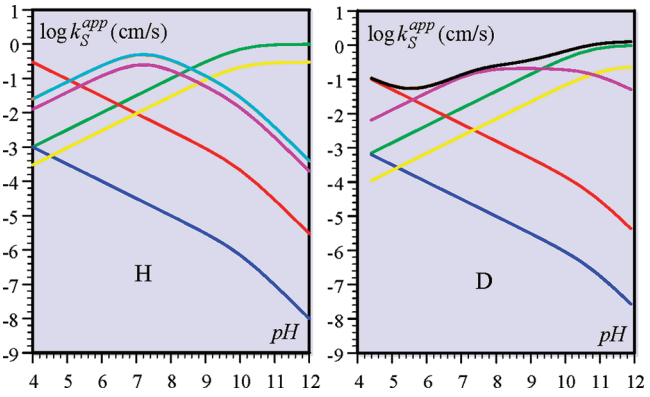

Figure 5. Contribution of the various pathways to the apparent standard rate constant (eq 2) as a function of pH (see text) in H_2O (left) and D_2O (right). Blue, EPT; green, PET; red, CPET−$H(D)_2O$; yellow, CPET−$H(D)O^-$; magenta, CPET−0.25 M $H(D)PO_4^{2-}$; cyan, CPET−0.5 M HPO_4^{2-}; black (right diagram), sum of all contributions.

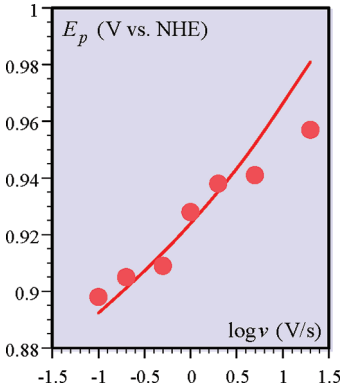

Figure 6. Cyclic voltammetry of 0.2 mM phenol in D_2O in a phosphate buffer at pD = p$K_{D_2PO_4^-}$ = 7.8 in the presence of 0.5 M KNO_3. Variation of the peak potential with the scan rate for 0.25 M buffer concentration. Full line represents simulation according to the mechanism in Scheme 2, in which H is replaced by D (see text and Table 1).

z being the charge number of the reactants,

$$w_R^Z = zF\phi_Z, \quad w_P^Z = (z+1)F\phi_Z$$

leading to

$$k_{S,\,corr}^{CPET-Z} = k_S^{CPET-Z} \exp\left[\frac{(2z+1)F\phi_Z}{2RT}\right] \qquad (4)$$

Further analysis of the kinetic data therefore requires the determination of the potential of the reaction sites and starting with the potential in the outer Helmoltz plane (OHP, see Scheme 3), traditionally noted ϕ_2, that is, the potential at the boundary between the compact double layer (portion of space between the electrode and the OHP) and the diffuse double layer (portion of space between the OHP and the solution).[15a] This potential may be obtained, in the framework of the Gouy−Chapman theory, from double layer capacitance data according to

$$\phi_2 = \frac{2RT}{zF}\,\mathrm{asinh}\left[\frac{C_d(E - E_{pzc})}{(8RT\varepsilon_0\varepsilon c)^{1/2}}\right] \qquad (5)$$

dx.doi.org/10.1021/ja206561n |J. Am. Chem. Soc. 2011, 133, 19160–19167

Scheme 3. Double Layer Effects

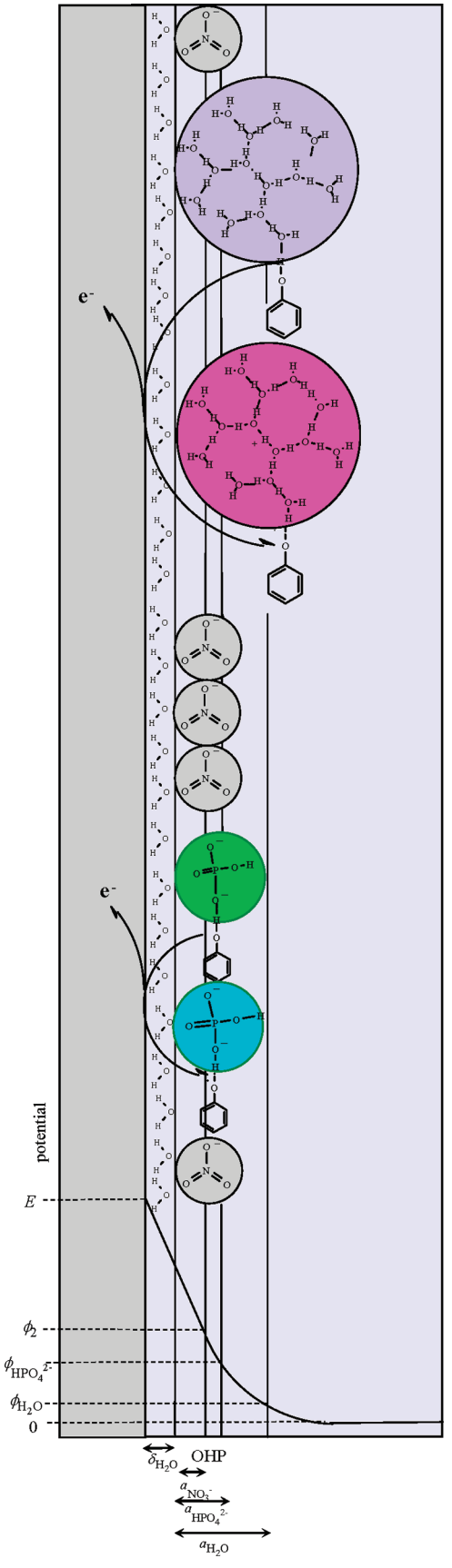

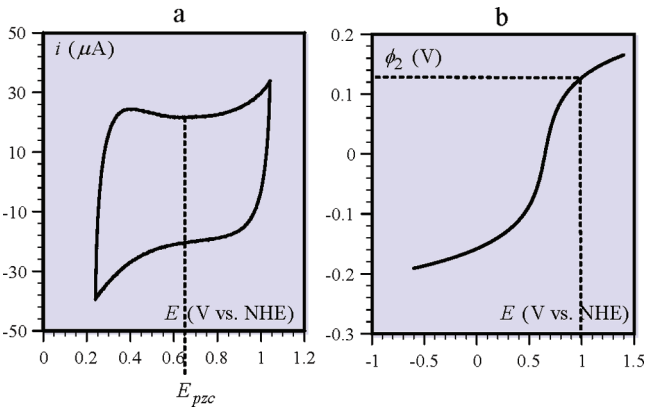

Figure 7. (a) Cyclic voltammetry of a solution in a 0.1 M phosphate buffer at pH = 7.2 in the presence of 0.5 M KNO_3 showing the double layer charging current in the region of the potential of zero charge, E_{pzc}. Scan rate = 2 V/s. (b) Variation of the outer Helmholtz plane potential with the electrode potential under the same conditions.

Table 2. Electrochemical Standard Rate Constants (cm s^{-1}) for Phenol Oxidation, Correction of Double Layer Effects

dimensions (Å)	$\delta_{H_2O} = 1.5$, $a_{NO_3^-} = 2.9$[16]
	$a_{HPO_4^{2-}} = 3.5$,[5b] $a_{H_2O} = 6.5$[5b]
	$\kappa^{-1} = 4.2$
potentials (V)	$\phi_2 = 0.125$
	$\phi_{HPO_4^{2-}} = 0.108$, $\phi_{H_2O} = 0.053$
raw standard rate constants	$k_{S,25°C}^{CPET-H_2O} = 25$, $k_{S,25°C}^{CPET-HPO_4^{2-}} = 1.1$
corrected standard rate constants	$k_{S,corr,25°C}^{CPET-H_2O} = 83$, $k_{S,corr,25°C}^{CPET-HPO_4^{2-}} = 0.002$

where z is the reactant electric charge ε_0 is the vacuum permittivity, ε is the dielectric constant of the solvent (here 78.8), c is the electrolyte concentration (here 0.5 M, the concentration of KNO_3 in excess over the other components of the solution), C_d is the differential capacity of the electrode, and E_{pzc} is the potential of zero charge. From the shallow minimum in Figure 7a, E_{pzc} = 0.65 vs NHE, and from the approximately constant anodic capacitive current, C_d = 150 μF/cm^2, application of eq 5 leads to an estimation of ϕ_2 as a function of the electrode potential (Figure 7b). In the zone of electrode potentials where the experiments were carried out, we may estimate that, on average, $\phi_2 \approx$ 0.125 V at the peak potential. In view of the radius of the nitrate ion and the radii of the proton in water and of hydrogen phosphate (Table 2), the potential at the reaction site (Scheme 3), ϕ_Z, is smaller than ϕ_2:[15a]

$$\phi_Z = \phi_2 \exp[-\kappa(a_Z - a_{NO_3^-})]$$

where κ^{-1} is the Debye length for the electrolyte concentration used in the experiments summarized in Figures 1−6 as reported in Table 2.

The resulting values of the potential at the reaction site for water and hydrogen phosphate are listed in Table 2, enabling the correction of the raw standard rate constants according to eq 4, and thus leading to the corrected values in Table 2.

Electrochemical Oxidation of Phenoxide Ion. The oxidation of phenoxide ion was investigated to have at disposal a reference ET reaction (Scheme 4) to be compared with the two CPET reactions. While an extensive investigation of the variations with temperature and scan rate was hampered in the case of phenol by the proximity of the oxidation wave to the discharge of the supporting electrolyte, this was possible in the present case

Scheme 4

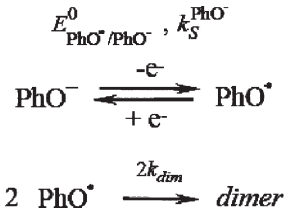

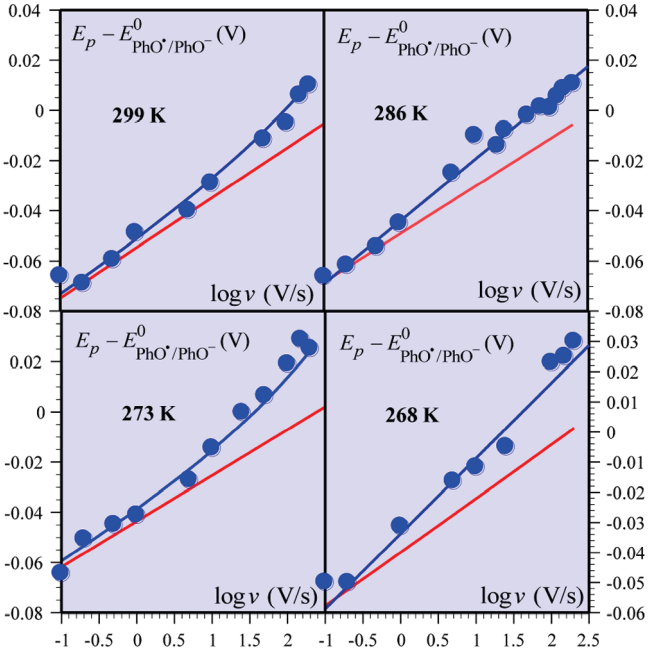

Figure 8. Oxidative cyclic voltammetry of a 0.2 mM phenol solution in a 0.1 M Britton buffer at pH = 12 in the presence of 0.5 M KNO_3, featuring the oxidation of phenoxide ion. Variation of the peak potential with the scan rate at various temperatures (number in each diagram), blue dots = experimental data, blue lines = simulation according to Scheme 4 with the parameter values listed in Table 3,[9] red lines = rate-determining dimerization.

since the oxidation of phenoxide ion is less positive. The results are shown in Figure 8 where the variations of the peak potential with scan rate at four temperatures are displayed as well as their simulations according to Scheme 4 so as to derive the values of the standard rate constants.

The resulting Arrhenius plot is displayed in Figure 9. The raw values of the standard rate constant were then corrected from double layer effects in the same way as for phenol oxidation, considering that the reaction site sits at the OHP and that ϕ_2 = 0.100 V on average in the potential domain where the oxidation peak of phenoxide ion is located, leading to the values listed in Table 3 and to a corrected Arrhenius plot (Figure 9).

DISCUSSION

A first observation upon perusal of Table 4 is that, in the CPET electrochemical oxidation of phenol, water (in water) is a much more efficient proton acceptor than hydrogen phosphate as far as corrected standard rate constants, that is, intrinsic

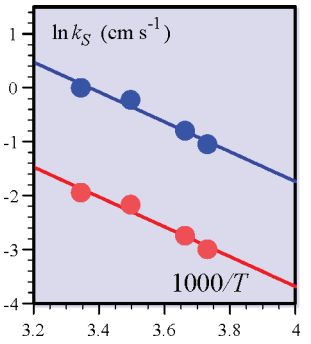

Figure 9. Oxidation of phenoxide ion. Arrhenius plots derived from the data in Figure 8, blue = raw data, red = corrected from double layer effects.

Table 3. Phenoxide Ion Oxidation, Correction of Double Layer Effects and Variations with Temperature

temp (K)	299	286	273	268
$D \times 10^5$ (cm^2 s^{-1}) [a]	2.7	2.5	1.4	1.1
$k_{dim} \times 10^{-9}$ (M^{-1} s^{-1}) [b]	1.3	0.9	0.6	0.4
$E^0_{PhO^\bullet/PhO^-}$ (V vs NHE) [c]	0.930	0.935	0.845	0.860
raw standard rate constant, $k_S^{PhO^-}$	1.00	0.80	0.45	0.35
corrected standard rate constant, $k_{S,corr}^{PhO^-}$	0.15	0.12	0.07	0.05

[a] From peak heights. [b] From the measured temperature dependence of the diffusion coefficient and the Debye−Smoluchowski relationship between bimolecular diffusion limit and the diffusion coefficient. [c] The standard potentials were obtained from the peak potential by the same procedure as depicted in Figure 1.

properties, are concerned. This observation parallels the comparison between the same two proton acceptors in homogeneous oxidation of phenol by photogenerated $Ru^{III}(bpy)_3^{5}$ when also made at zero driving force and in which the effect of electrostatic work terms has also been corrected (Table 4). The H_2O/HPO_4^{2-} rate ratio is however substantially bigger in the electrochemical case than in the homogeneous case. These observations call for a more quantitative analysis of the comparison between the electrochemical and homogeneous reactions.

The corrected electrochemical standard rate constants may be expressed as:[17]

$$k_{S,corr}^{CPET-Z} = Z_{el}^{CPET-Z} \frac{\pi \exp\left[-\dfrac{\lambda_{el}^{CPET-Z}}{4RT}\right]}{\sqrt{1 + \dfrac{\pi RT}{\lambda_{el}^{CPET-Z}}}}$$

after introduction of the reorganization energy, λ_{el}^{CPET-Z}, and of the pre-exponential factor, Z_{el}^{CPET-Z} (Z being either water or hydrogen phosphate). The electrochemical reorganization energy may be derived from the homogeneous self-exchange reorganization energy, taking into account image force effects according to[18]

$$\lambda_{el}^{CPET-Z} = \lambda_{se}^{CPET-Z}\left(1 - \frac{a_Z}{d_Z}\right)$$

where a_Z is the radius of the equivalent sphere and $d_Z = 2(\delta_{H_2O} + a_Z)$, the distance between the reaction site and its electrical image (see

dx.doi.org/10.1021/ja206561n |J. Am. Chem. Soc. 2011, 133, 19160–19167

Table 4. Electrochemical[a] and Homogeneous[b] Kinetic Characteristics[c]

electrochemical	homogeneous[5]
$k_{S,corr,25°C}^{CPET-H_2O} = 83$	$k_{0,25°C}^{CPET-H_2O} = 8.8 \times 10^7$ [d]
$k_{S,corr,25°C}^{CPET-HPO_4^{2-}} = 0.002$	$k_{0,25°C}^{CPET-HPO_4^{2-}} = 2 \times 10^4$
$\frac{k_{S,corr,25°C}^{CPET-H_2O}}{k_{S,corr,25°C}^{CPET-HPO_4^{2-}}} = 3.9 \times 10^4$	$\frac{k_{0,25°C}^{CPET-H_2O}}{k_{0,25°C}^{CPET-HPO_4^{2-}}} = 4.4 \times 10^3$
$KIE_{el,25°C}^{CPET-H_2O} = 2.75$ [e]	$KIE_{hom,25°C}^{CPET-H_2O} = 4.0$
$KIE_{el,25°C}^{CPET-HPO_4^{2-}} = 2.4$ [e]	$KIE_{hom,25°C}^{CPET-HPO_4^{2-}} = 3.5$
$\lambda_{el}^{CPET-H_2O} = 0.27$ [f]	$\lambda_{se}^{CPET-H_2O} = 0.45$ eV
$\lambda_{el}^{CPET-HPO_4^{2-}} = 0.56$ [f]	$\lambda_{se}^{CPET-HPO_4^{2-}} = 0.86$ eV
$Z_{el}^{CPET-H_2O} = 390$ cm s^{-1}	$Z_{hom}^{CPET-H_2O} = 1.2 \times 10^{10}$
$Z_{el}^{CPET-HPO_4^{2-}} = 0.16$ cm s^{-1}	$Z_{hom}^{CPET-HPO_4^{2-}} = 2 \times 10^7$ M s^{-1}
$\log\left(\frac{Z_{el}^{CPET-H_2O}}{Z_{el}^{CPET-HPO_4^{2-}}}\right) = 3.4$	$\log\left(\frac{Z_{hom}^{CPET-H_2O}}{Z_{hom}^{CPET-HPO_4^{2-}}}\right) = 2.8$
$\lambda_{el}^{ET-PhO^-} = 1.1$ eV	
$Z_{el}^{ET-PhO^-} = 8 \times 10^4$ cm s^{-1}	

[a] Standard rate constants in cm s^{-1}. [b] Rate constants in M^{-2} s^{-1}. [c] Energies in eV. [d] Taking into account image force effects with d_{H_2O} = 16, $d_{HPO_4^{2-}}$ = 10 Å (see text). [e] From the ratio of the uncorrected standard rate constants in Table 1. [f] corrected from work terms.

Scheme 3). The ensuing reorganization energies for water and hydrogen phosphate are reported in Table 4, as well as the values of the pre-exponential factor. It is again observed, as in the homogeneous case, that the pre-exponential factor is substantially larger in the case of water than in the case of hydrogen phosphate.

The electrochemical results thus confirm the very peculiar nature of water (in water) as a proton acceptor previously characterized in the homogeneous oxidation of phenol: the charge of the proton generated in the reaction is delocalized over a large cluster of water molecules; the electron transfer reaction is concerted with Grotthus-type proton displacements by means of H-bond relays.

It is worth noting that the H_2O/HPO_4^{2-} ratio of pre-exponential factors is, after all work term corrections have been made, substantially larger, by a factor of ca. 10, in the electrochemical case than in the homogeneous case. A likely reason for this difference is the existence of an electric field effect in the reaction site favoring the zwitterionic form of the reactant system in the transition state, (PhO^-,H^+nH_2O), as already observed in the oxidation of an aminophenol in which the proton acceptor is an internal base.[19] The observation that the H/D kinetic isotope effect (Table 3) is smaller in the electrochemical case (2.4−2.75) than in the homogeneous case (3.5−4.0) can be interpreted as an additional manifestation of the same phenomenon.

An additional source of information is provided by comparing the electrochemical CPET reactions with the oxidation of phenoxide ion taken as a reference ET reaction, for which the reorganization energy and the pre-exponential factor could be derived from temperature-dependent experiments,[20] leading to the values reported in Table 3. It is interesting to note that the pre-exponential factor 8×10^4 cm s^{-1}, is substantially larger than the collision frequency, $[RT/(2\pi M)]^{1/2} = 6.5 \times 10^3$ cm s^{-1} (M = molar mass) for phenoxide ion, which may be attributed to the fact that the electron transfer reaction starts to take place before the reactant has reached the outer Helmholtz plane as discussed earlier.[17,19]

The pre-exponential factors found for the HPO_4^{2-}− and H_2O−CPET reactions are much smaller, by a factor of 5×10^5 in the first case and 205 in the second. This considerable decrease of the pre-exponential factor when passing from a simple ET reaction to the CPET reactions indicates that, in the later case, the pre-exponential factor is not simply a combined measure of proton tunneling (in which case, the KIE should be very large) and structureless approach of the two reactants, phenol and proton acceptor, assimilated to spheres, toward the electrode surface as sketched in Scheme 3. The precursor complex is actually likely to adopt a precise spatial structure so as to allow the formation of one or several H-bonds as required by the occurrence of the CPET reaction, thus decreasing considerably the number of efficient collisions.

CONCLUDING REMARKS

The CPET oxidation of phenol with water (in water) and hydrogen phosphate as proton acceptors has provided a good example for testing the consistency of the electrochemical and homogeneous approaches to a reaction, the comprehension of which raises more mechanistic and kinetic challenges than that of a simple outer-sphere electron transfer. In terms of driving forces, hydrogen phosphate is a better proton acceptor than water (by ca. 0.4 eV), but when comparison is made at zero driving force, water (in water) appears as more efficient than hydrogen phosphate. This observation, originally derived from homogeneous experiments, is confirmed by the value found for the electrochemical standard rate constants. A meaningful comparison between the electrochemical and homogeneous intrinsic properties requires correcting the raw data from electrical work terms. In the first case, this operation consisted in correcting from the effect of the electrochemical double layer at the level of the reaction site. This estimate was based on the reactant dimensions revealed by the analysis of the homogeneous results. This is also the case for the evaluation of the electrochemical reorganization energy, derived from a detailed analysis of a large set of homogeneous experiments carried out as a function of temperature, while analogous electrochemical experiments could not be performed. Once the electrochemical reorganization energy was thus determined, the electrochemical pre-exponential factors could be obtained and compared with their homogeneous counterparts. The intrinsic advantage of water (in water) over hydrogen phosphate is therefore confirmed, corroborating the mechanism by which electron transfer is concerted with Grotthus-type proton translocation in water. More precise comparison between the pre-exponential factors and H/D kinetic isotope effects revealed that electric field effects that favor zwitterionic forms in the transition state may be at work in the electrochemical case. The electrochemical oxidation of phenoxide ion could be investigated as a function of temperature, providing a detailed picture of a system that can be used as a reference outersphere electron transfer to be compared with the CPET reactions. The huge decrease of the pre-exponential thus observed points to a CPET precursor complex that possesses a precise spatial structure allowing the formation of one or several H-bonds as required by the occurrence of the CPET reaction, thus decreasing considerably the number of efficient collisions compared with those undergone by structureless spherical reactants.

In summary, consistency between the two approaches of the same reaction is indeed observed after some specific, and rather modest, effects, such as electric field effects, have been taken into account. One worth noting consequence is the possibility of transferring information from one domain to the other so as to obtain a deeper comprehension of the reaction.

■ ASSOCIATED CONTENT

Supporting Information. Experimental details, proof of eq 2, details of ref 16. This material is available free of charge via the Internet at http://pubs.acs.org.

■ AUTHOR INFORMATION

Corresponding Author
saveant@univ-paris-diderot.fr

■ REFERENCES

(1) Proton-Coupled Electron Transfer. Thematic Issue. *Chem. Rev.* **2010**, *110*, 6937−7100.

(2) Not all PCET literature uses the same symbolism, calling for a careful attention to the acronym definitions in each case.

(3) (a) Reece, S. Y.; Nocera, D. G. *Annu. Rev. Biochem.* **2009**, *78*, 33.1. (b) Dempsey, J. L.; Winkler, J. R.; Gray, H. B. *Chem. Rev.* **2010**, *110*, 7024.

(4) (a) Despite passing from cyclic voltammetry to slightly different techniques, normal pulse voltammetry, differential pulse voltammetry, second harmonic AC voltammetry, etc. With the same characteristic time, all techniques are equivalent as far as making diffusion faster than the decay of the first intermediate, therefore rendering the electrochemical response chemically reversible. For example, a 60 hertz frequency in AC voltammetry corresponds to a scan rate of 1.5 V/s. Proof of chemical reversibility is less obvious with these techniques than with cyclic voltammetry, making artifactual mistakes easy to occur.[4b,c] (b) Andrieux, C. P.; Hapiot, P.; Pinson, J.; Savéant, J.-M. *J. Am. Chem. Soc.* **1993**, *115*, 7783. (c) Savéant, J.-M. *Elements of Molecular and Biomolecular Electrochemistry*; Wiley-Interscience: New York, 2006.

(5) (a) Bonin, J.; Costentin, C.; Louault, C.; Robert, M.; Routier, M.; Savéant, J.-M. *Proc. Natl. Acad. Sci. U.S.A.* **2010**, *107*, 3367. (b) Bonin, J.; Costentin, C.; Louault, C.; Robert, M.; Savéant, J.-M. *J. Am. Chem. Soc.* **2011**, *133*, 6668.

(6) Costentin, C.; Louault, C.; Robert, M.; Savéant, J.-M. *Proc. Natl. Acad. Sci. U.S.A.* **2009**, *106*, 18143.

(7) (a) For early studies of the electrochemical oxidation of phenols, see ref 7b,c. (b) Richards, J. A.; Whitson, P. E.; Evans, D. H. *J. Electroanal. Chem.* **1975**, *63*, 311. (c) Speiser, B.; Rieker, A. *J. Electroanal. Chem.* **1979**, *193*, 373.

(8) Ye, M.; Schuler, R. H. *J. Phys. Chem.* **1989**, *93*, 1898.

(9) Rudolph, M. *J. Electroanal. Chem.* **2003**, *543*, 23.

(10) Dixon, W. T.; Murphy, D. *J. Chem. Soc., Faraday Trans. 1* **1976**, *72*, 1221.

(11) (a) *Handbook of Chemistry and Physics*, 82nd ed.; Lide, D. R., Ed.; CRC Press: Boca Raton, FL, 2001−2002; pp 8−45, (b) pp 8−49.

(12) Gary, R.; Bates, R. G.; Robinson, R. A. *J. Phys. Chem.* **1964**, *68*, 3806.

(13) Tripathi, G. N. R.; Schuler, R. H. *J. Chem. Phys.* **1984**, *81*, 113.

(14) Krezel, A.; Bal, W. *J. Inorg. Biochem.* **2004**, *98*, 161.

(15) (a) Delahay, P. *Double Layer and Electrode Kinetics*; Interscience: New York, 1965. (b) Application of the Gouy−Chapman model of the electrochemical double layer has long be restricted to mercury electrodes, until recent careful and convincing application to glassy carbon electrodes.[15c] (c) Meneses, A. B.; Antonello, S.; Arvalo, M. C.; Maran, F. *Electroanalysis* **2006**, *18*, 363.

(16) Frisch, M. J., et al. *Gaussian*, revision C.02; Gaussian, Inc.: Wallingford CT, 2004.

(17) Feldberg, S. W.; Sutin, N. *Chem. Phys.* **2006**, *324*, 216.

(18) (a) Marcus, R. A. *J. Chem. Phys.* **1965**, *43*, 670. (b) Hush, N. S. *Electrochim. Acta* **1968**, *13*, 1005.

(19) Costentin, C.; Robert, M.; Savéant, J.-M. *Phys. Chem. Chem. Phys.* **2010**, *12*, 13061.

(20) This was not feasible in the homogeneous case because of a side reaction between phenoxide ion and methylviologen serving as quencher of the excited $Ru^{II}(bpy)_3$ complex.